TNP-ATP and TNP-ADP as Probes of the Nucleotide Binding Site of CheA, the Histidine Protein Kinase in the Chemotaxis Signal Transduction Pathway of *Escherichia coli*†

Richard C. Stewart,*,‡ Ricaele VanBruggen,‡ Dolph D. Ellefson,§,|| and Alan J. Wolfe§

Department of Cell Biology & Molecular Genetics, University of Maryland, College Park, Maryland 20742, and Department of Microbiology & Immunology, Loyola University Chicago, Maywood, Illinois 60153

Received April 29, 1998; Revised Manuscript Received June 30, 1998

ABSTRACT: The interaction of CheA with ATP has important consequences in the chemotaxis signal transduction pathway of *Escherichia coli*. This interaction results in autophosphorylation of CheA, a histidine protein kinase. Autophosphorylation of CheA sets in motion a chain of biochemical events that enables the chemotaxis receptor proteins to communicate with the flagellar motors. As a result of this communication, CheA allows the receptors to control the cell swimming pattern in response to gradients of attractant and repellent chemicals. To probe CheA interactions with ATP, we investigated the interaction of CheA with the fluorescent nucleotide analogues TNP-ATP [2′(3′)-*O*-(2,4,6-trinitrophenyl)adenosine 5′-triphosphate] and TNP-ADP. Spectroscopic studies indicated that CheA bound TNP-ATP and TNP-ADP with high affinity (micromolar K_d values) and caused a marked enhancement of the fluorescence of the TNP moiety of these modified nucleotides. Analysis of titration experiments indicated a binding stoichiometry of two molecules of TNP-ATP (TNP-ADP) per CheA dimer and suggested that the two binding sites on the CheA dimer operate independently. Binding of TNP-ATP to CheA was inhibited by ATP, and analysis of this inhibition indicated that the CheA dimer binds 2 molecules of ATP. Competition experiments also indicated that CheA binds TNP-ATP considerably more tightly than it binds unmodified ATP. Binding of TNP-ADP to CheA was inhibited by ADP in a similar manner. TNP-ATP was not a substrate for CheA and served as a potent inhibitor of CheA autophosphorylation (K_i < 1 μM). The glycine-rich regions (G1 and G2) of CheA and other histidine protein kinases have been presumed to play important roles in ATP binding and/or catalysis of CheA autophosphorylation, although few experimental tests of these functional assignments have been made. Here, we demonstrate that a CheA mutant protein with Gly→Ala substitutions in G1 and G2 has a markedly reduced affinity for ATP and ADP, as measured by Hummel−Dreyer chromatography. This mutant protein also bound TNP-ATP and TNP-ADP very poorly and had no detectable autokinase activity. Surprisingly, a distinct single-site substitution in G2 (Gly470→Lys) had no observable effect on the affinity of CheA for ATP and ADP, despite the fact that it rendered CheA completely inactive as an autokinase. This mutant protein also bound TNP-ATP and TNP-ADP with affinities and stoichiometries that were indistinguishable from those observed with wild-type CheA. These results provide some preliminary insight into the possible functional roles of G1 and G2, and they suggest that TNP-nucleotides are useful tools for exploring the effects of additional mutations on the active site of CheA.

A large number of two-component sensory response pathways have been identified in recent years. Although the cataloging of such systems is still incomplete, current information indicates that the two-component signaling paradigm is used extensively and in a wide variety of organisms including numerous prokaryotes, several archeons, and at least some eukaryotic organisms (*1*−*7*). While the details of the signaling circuitry can vary from one system to another, each such pathway utilizes two key components: a histidine protein kinase (HPK) and a cognate phospho-accepting response regulator protein (RR) (*1*, *4*, *9*). The HPK autophosphorylates at a specific histidine residue; this phosphoryl group is then transferred to the RR, causing a conformational change that alters RR activity in a manner that elicits an appropriate response. Comparisons of the amino acid sequences of large numbers of HPKs have revealed several conserved features that are thought to play key roles in binding ATP and catalyzing phosphorylation of a specific histidine side chain in each HPK. Among these conserved elements are two distinct glycine-rich regions (called G1 and G2) and two other segments referred to as N and F. These 4 short blocks of common sequence (5−12 residues each) are embedded in a larger segment of ∼200 residues referred to as the 'transmitter module' (*4*, *9*). Similar sequence comparisons in the RR superfamily have indicated that each RR protein includes a conserved 'receiver module' that interacts with the appropriate cognate HPK to

† This research was supported by U.S. Public Health Service Grants GM52583 to R.C.S. and GM46221 to A.J.W.

* Corresponding author. Phone: (301) 405-5475. FAX: (301) 314-9489. Email: rs224@umail.umd.edu.

‡ University of Maryland.

§ Loyola University Chicago.

|| Present address: Department of Microbiology & Immunology, Oregon Health Scienes University, Portland, OR 97201.

S0006-2960(98)00970-2 CCC: $15.00
Published on Web 08/07/1998

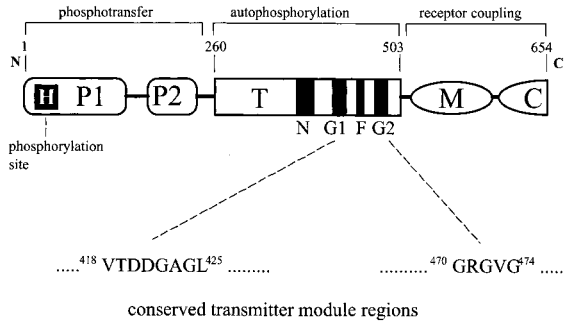

FIGURE 1: Functional organization of CheA. P1, P2, T, M, and C are regions defined as discrete structural and/or functional domains by a variety of different approaches (*4*, *17*−*20*). Within the T (transmitter) domain, there are four blocks of amino acids that are conserved in two-component histidine protein kinases. These blocks are designated N, G1, F, and G2 (*4*).

acquire the histidine-phosphoryl group from this HPK. This interaction results in phosphorylation of the RR on a conserved aspartyl side chain (*8*), and this modification controls the activity of the RR (*4*, *9*).

In the chemotaxis system of *Escherichia coli*, *Salmonella typhimurium*, *Bacillus subtilis*, and other bacteria, the HPK CheA autophosphorylates and then passes its phosphoryl group to the RR protein CheY (*4*, *10*, *11*). Phospho-CheY, in turn, interacts directly with the flagellar motor to alter the frequency of CW flagellar rotation (*12*). The intracellular level of phospho-CheY reflects the relative rates of CheY phosphorylation (by CheA) and CheY dephosphorylation (assisted by CheZ) (*10*). By controlling the level of phospho-CheY in response to environmental gradients of nutrients and other chemicals (*13*, *14*), these bacteria can control their swimming patterns such that they migrate toward locations where the concentrations of attractant chemicals are higher and the concentrations of repellent chemicals are lower (*15*−*17*).

CheA comprises several distinct structural and functional domains (*4*, *17*−*20*), including a 240 amino acid transmitter module (Figure 1). This region of the protein encompasses the kinase active site of CheA and, therefore, is sometimes referred to as the catalytic domain (*21*). This domain is responsible for binding ATP and catalyzing transfer of the ATP γ-phosphoryl group to His^{48} located in the N-terminal P1 module. The catalytic domain of CheA includes the four conserved elements common to most HPK transmitter modules (N, G1, F, and G2). These short blocks are thought to function as key elements for the interaction of CheA with ATP and catalysis of autophosphorylation. G1 and G2, in particular, have been proposed to function in ATP binding (*4*, *17*) because of their similarities to glycine-rich regions of other nucleotide binding proteins (*22*−*25*). Recent work has established that mutations in the G1 and G2 regions of CheA eliminate CheA autokinase activity in vitro and, therefore, abolish chemotaxis ability in vivo (*26*). However, these studies did not examine whether G1 and G2 mutations specifically disrupted the ATP binding ability of CheA.

Similar work has established that some of the conserved elements of the transmitter module are important for HPK autokinase activity in a variety of other two-component systems (*4*, *27*, *28*). However, it is important to note that loss of autokinase activity in such mutant HPKs does not necessarily implicate the mutated positions in ATP binding per se. Loss of activity could just as easily arise from the following: disruption of active site elements involved in promoting the chemistry of phosphotransfer from ATP to histidine; loss of the ability to orient the phospho-accepting histidine relative to the active site; or loss of HPK dimerization. Ninfa et al. (*27*) used UV cross-linking of bound ATP as an approach to investigate whether mutations in several conserved transmitter positions affected ATP binding in the histidine protein kinase NR_{II}. To our knowledge, this is the only published work that specifically examined nucleotide binding, as opposed to kinase activity, for a mutant HPK. In the work reported here, we adopted an alternative approach for exploring ATP binding by CheA.

Although recent work has provided some insight into the CheA autophosphorylation reaction (*20*, *21*, *29*−*33*), several fundamental questions concerning CheA's autokinase mechanism remain unanswered. Many of these questions arise from the dimeric nature of CheA (*34*): CheA monomers are incapable of autophosphorylation, but, at sufficiently high concentrations, these monomers readily dimerize to generate the catalytically active kinase (*30*). If the CheA dimer is symmetric, it is possible that each dimer has two kinase active sites. However, the actual number of ATP binding sites per CheA dimer has not yet been established experimentally, and binding studies to investigate the possibility of cooperative interactions between binding sites in a CheA dimer have not been possible. Previous efforts to monitor ATP binding by CheA (*31*) utilized the chromatographic approach of Hummel and Dreyer (*35*). Although such experiments helped to define the approximate affinity of CheA for ATP and ADP, they did not enable unambiguous determination of the binding stoichiometry, nor did they provide data of sufficient quality to address the possibility of cooperativity. In the work presented here, we investigated the ability of TNP-ATP and TNP-ADP to interact with CheA. These fluorescent nucleotide analogues provided sensitive spectrophotometric probes of CheA−nucleotide binding and enabled us to define the stoichiometry of binding. In addition, we utilized these probes to characterize the effects of two mutations in the CheA transmitter module.

EXPERIMENTAL PROCEDURES

Materials. 2′(3′)-*O*-(2,4,6-Trinitrophenyl)adenosine 5′-triphosphate (TNP-ATP) and 2′(3′)-*O*-(2,4,6-trinitrophenyl)-adenosine 5′-diphosphate (TNP-ADP) were purchased from Molecular Probes, Inc. (Eugene, OR), stored at −20 °C in the dark, and utilized under minimal lighting conditions. Concentrations of TNP-ATP and TNP-ADP were determined spectrophotometrically based on the extinction coefficient of 26.4 mM^{-1} cm^{-1} at 408 nm (*36*). ADP and high-purity ATP were purchased from Pharmacia and Boehringer Mannheim. All other chemicals were reagent grade and were purchased from standard commercial sources.

Mutant Variants of CheA. In CheA-H48Q, the site of autophosphorylation (His^{48}) has been altered to a nonphosphorylatable amino acid. CheA-G1/G2 carries the following four amino acid changes: Gly^{422}→Ala, Gly^{470}→Ala, Gly^{472}→Ala, Gly^{474}→Ala. CheA-G470K is one of the original mutant proteins ('CheA-501') generated in the Simon laboratory by random mutagenesis and characterized by Oosawa et al. (*11*); in this mutant protein, Gly^{470} has been changed to Lys (note

that this mutation in G2 differs from the Gly→Ala substitutions in CheA-G1/G2). Previous publications specify the details concerning the construction of these mutants and of the expression vectors used to overproduce the respective proteins (*26*, *33*).

Bacterial Strains and Plasmids. Ampicillin was added to an initial concentration of 100 μg/mL for growth of cell/plasmid cultures. *E. coli* strain BL21(DE3) (*37*) was used for expression of $(His)_6$-tagged CheA variants and for production of CheY using pT7:cheY (*38*). The following CheA variants were expressed with N-terminal $(His)_6$ tags using the parent expression plasmid pET14b (Novagen Inc., Madison, WI): wild-type CheA, CheA-H48Q, CheA-G470K, and CheA-G1/G2. Wild-type CheA lacking the $(His)_6$ tag was purified using expression vector pAR1:cheA (*33*) in *E. coli* strain RP3098 [Δ(*flhA-flhD*), kindly provided by J. S. Parkinson, University of Utah]. In numerous TNP-ATP titration experiments, $(His)_6CheA^{wt}$ and $CheA^{wt}$ lacking the $(His)_6$ tag performed identically, suggesting that the N-terminal $(His)_6$ tag had no effect on the interactions of CheA with ATP and TNP-ATP (data not shown).

Protein Purification. Wild-type CheA and CheY were purified following procedures published previously (*33*). Purification of $(His)_6$-tagged CheA variants followed the same AffiGel Blue and DEAE-cellulose chromatography steps as for untagged CheA, but also included Ni−NTA column chromatography as a final step (Qiagen Inc., Santa Clarita, CA). Proteins were concentrated to approximately 50−100 μM and stored at −80 °C in TEGDK buffer (*10*). CheA samples were dialyzed against TEDK buffer (*31*) immediately before use. Where indicated, $MgCl_2$ was added to CheA samples to give a final concentration of 10 mM immediately before use; in these cases, the buffer is referred to as TEDKM. Concentrations of purified proteins were determined spectrophotometrically using extinction coefficients calculated following the method of Gill and von Hippel (*39*). All CheA concentrations are specified as the concentration of CheA monomer equivalents.

Assays of CheA Activity. Steady-state turnover of CheA (results presented in Figures 9A and 10A) was monitored using a coupled ATPase system (*40*) as described by Ninfa et al. (*13*) and Lukat et al. (*44*). Reactions contained 2 μM CheA, 10 μM CheY, 1 mM phosphoenolpyruvate, 0.2 mM NADH, 10 units/mL pyruvate kinase, and 30 units/mL lactate dehydrogenase (Boehringer Mannheim) in TEDKM buffer (*31*). This coupling system enabled spectrophotometric monitoring of ATP consumption by following the rate of oxidation of NADH to NAD^+ ($\Delta\epsilon_{340} = 6.2\ mM^{-1}\ cm^{-1}$). Control experiments indicated that the coupling system was not inhibited by either TNP-ATP or TNP-ADP in the concentration ranges used in this work. This was tested by adding small amounts of ADP into the coupling mixture in the presence or absence of TNP-nucleotide and then observing the resulting ΔA_{340}. The TNP-nucleotides did not affect the magnitude of the observed ΔA_{340}, and these A_{340} changes were complete within the time it took to mix the cuvette contents and close the lid of the spectrophotometer (∼5 s). Steady-state turnover of CheA was also monitored using an enzymatic P_i detection system (*42*) purchased from Molecular Probes, Inc., Eugene, OR. Results with this alternative system paralleled those obtained with the NADH-coupled system (data not shown) and also indicated that TNP-ATP does not serve as a substrate for CheA under our conditions.

Fluorescence Measurements. Samples were prepared in TEDKM buffer in standard 1 cm × 1 cm fluorescence cuvettes maintained at 25 °C. Fluorescence emission spectra were recorded using a Jobin Yvon-Spex Fluromax-2 spectrofluorometer with the excitation wavelength set at 410 nm and the emission wavelength scanned from 480 to 650 nm. Excitation and emission monochromators were set to give a slit width of 4 nm. For analysis of titration data, the observed emission intensity of each sample (at 541 nm) was corrected by subtraction of the signal observed with an appropriate blank: buffer plus TNP-ATP or buffer plus TNP-ADP. A 'no CheA' blank titration was performed for each CheA titration experiment. Therefore, the observed fluorescence change (ΔF_{obs}) plotted in Figures 3−8 represents the enhancement of fluorescence emission intensity (ΔF at 541 nm) due to formation of the complex between CheA and the TNP-modified nucleotide. In the absence of CheA, TNP-ATP and TNP-ADP samples had fluorescence emission intensities that were proportional to the nucleotide concentration up to a concentration of 1 μM. At higher TNP-nucleotide concentrations, inner filter effects caused this relationship to deviate from linearity. This effect required us to apply a correction factor to the fluorescence data collected at TNP-nucleotide concentrations higher than 1 μM. This correction factor was calculated by determining the ratio of the theoretical fluorescence intensity (predicted by extrapolating the linear region of plots) to the actual observed fluorescence intensity (*43*).

The CheA concentrations chosen for most of the experiments reported here were about 1 μM (monomer equivalents). This choice represents a compromise between two opposing considerations: (i) to generate the most useful binding isotherms, it was desirable to use protein concentrations that were close to the K_d of the ligand of interest (<1 μM); and (ii) to avoid possible complications arising from mixtures of CheA monomers and CheA dimers, it was desirable to use a relatively high protein concentration (>1 μM) to ensure that most of the CheA was present in a dimeric state. In analyzing our results, we assumed that all of the CheA was present in the dimeric form for CheA concentrations higher than 0.75 μM. Surette et al. (*30*) measured a K_d of 0.2−0.4 μM for dimer−monomer equilibrium for CheA from *S. typhimurium*. Our own measurements (data not shown) indicated an upper limit of 0.05−0.10 μM for the K_d the *E. coli* CheA dimer under our experimental conditions (TEDKM buffer). This K_d value predicts that, at a minimum, over 80% of the CheA would be present as the dimer at a total CheA concentration of 0.75 μM. In addition, our measurements of the turnover number of CheA at a series of CheA concentrations (0.02−5 μM) indicated that there was no detectable difference (±10%) between the turnover number observed at 0.75 μM CheA compared to that at 5 μM CheA, again supporting the idea that virtually all of the CheA was present in the active dimeric form at concentrations higher than 0.75 μM. Previous work has shown that phosphorylation of CheA and the presence of ATP have no effect on the monomer−dimer equilibrium (*30*).

Analysis of Fluorescence Titration Data To Determine Thermodynamic Binding Isotherms. As described above, we measured the binding of TNP-ATP and TNP-ADP to CheA by following the enhanced fluorescence emission of the

bound TNP-nucleotide. The ultimate goal of this work was to extract binding parameters (K_d values) from these data. To achieve this goal, we first had to define the relationship between the fluorescence change and nucleotide binding. This was accomplished following the general approach described by Bujalowski et al. (*44*, *45*). Specifically, we titrated three different concentrations of CheA with TNP-ATP and TNP-ADP. These data defined three saturation curves that were plotted as $\Delta F_{obs}/\Delta F_{total}$ versus the total concentration of added nucleotide. ΔF_{obs} is the observed fluorescence signal following nucleotide addition (corrected, as described above, for inner filter effects, for dilution effects, and for the signal observed at that nucleotide concentration in the absence of CheA). ΔF_{total} is the maximal value of ΔF_{obs} obtained at saturation. Using these saturation curves, the relationship between $\Delta F_{obs}/\Delta F_{total}$ and the amount of nucleotide bound per CheA dimer was defined as described previously (*44*, *45*). For any given value of $\Delta F_{obs}/\Delta F_{total}$ on any of these three saturation curves:

$$[\text{nucleotide}]_{total} = [\text{nucleotide}]_{free} + [\text{CheA dimer}][\text{nucleotide}]_{bound}/[\text{CheA dimer}] \quad (1)$$

Therefore, for each chosen value of $\Delta F_{obs}/\Delta F_{total}$, a plot of $[\text{nucleotide}]_{total}$ versus $[\text{CheA dimer}]$ had a slope equal to $[\text{nucleotide}]_{bound}/[\text{CheA dimer}]$. By determining the value of this slope at a series of different values of $\Delta F_{obs}/\Delta F_{total}$ (ranging from 0.05 to 0.92), we defined the relationship between $\Delta F_{obs}/\Delta F_{total}$ and $[\text{nucleotide}]_{bound}/[\text{CheA dimer}]$ (plotted in Figures 4B and 5B). Extrapolating this relationship to $\Delta F_{obs}/\Delta F_{total} = 1$ indicated the stoichiometry of the CheA−nucleotide interaction. In addition, the curve defined by the plot of $\Delta F_{obs}/\Delta F_{total}$ versus $[\text{nucleotide}]_{bound}/[\text{CheA dimer}]$ allowed us to generate a true binding isotherm from fluorescence data derived from any titration of CheA with TNP-nucleotide (*44*).

The binding isotherms generated in this way were fit (nonlinear least-squares) using eq 2 to determine the best-fit values of K_{d1} and K_{d2}:

$$[\text{nucleotide}]_{bound}/[\text{CheA dimer}] = N_f(K_{d2} + 2N_f)/[(K_{d1}K_{d2}) + (K_{d2}N_f) + N_f^2] \quad (2)$$

In this equation, K_{d1} represents the dissociation constant for the complex of the first molecule of nucleotide to a CheA dimer, K_{d2} represents the dissociation constant for the second molecule of nucleotide to this same dimer, and N_f represents the concentration of free nucleotide. If site 1 and site 2 are identical, noninteracting sites, then statistical factors dictate that $K_{d2} = 4K_{d1}$.

The dissociation constants for the complex of CheA with unmodified (nonfluorescent) ATP and ADP were determined using binding competition experiments in which CheA was titrated with TNP-nucleotide in the presence of various concentrations of ATP or ADP (Figures 7 and 8). The results of these titrations were analyzed using the same approach as outlined above for the titrations performed in the absence of inhibitor. The K_{d1} and K_{d2} values extracted from the binding isotherms were then further analyzed using eq 3:

$$\text{apparent } K_d^{TNP-ATP} = K_d^{TNP-ATP}(1 + [\text{ATP}]/K_d^{ATP}) \quad (3)$$

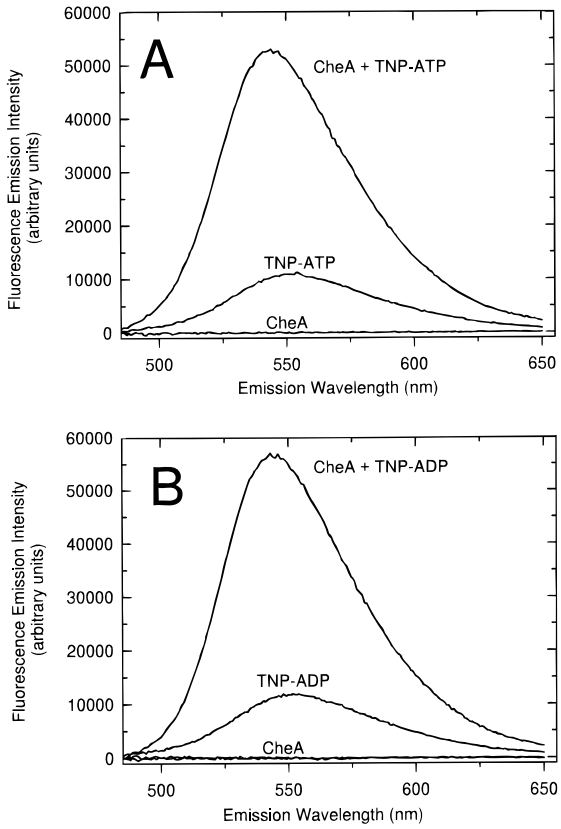

FIGURE 2: Fluorescence emission of TNP-ATP and TNP-ADP in the presence and absence of CheA. (A) The fluorescence emission spectrum of 0.8 μM TNP-ATP was recorded in the absence and presence of 1.0 μM CheA-H48Q. The excitation wavelength was 410 nm. The base line spectrum shows the emission spectrum for CheA in the absence of TNP-ATP. This spectrum was almost identical to that observed for buffer alone. (B) The fluorescence emission spectrum of 1.0 μM TNP-ADP was recorded in the absence and presence of 1.0 μM CheA-H48Q.

This relationship indicates that a plot of the apparent $K_d^{TNP-ATP}$ versus [ATP] should be linear with a *y*-axis intercept of $K_d^{TNP-ATP}$ and a slope of $K_d^{TNP-ATP}/K_d^{ATP}$. Therefore, the value of K_d^{ATP} can be calculated as the ratio of the *y*-axis intercept to the slope.

RESULTS

Characterization of CheA Interaction with TNP-ATP and TNP-ADP by Fluorescence Spectroscopy. Previous work demonstrated that TNP-ATP and TNP-ADP are weakly fluorescent in aqueous solutions and that this fluorescence can be enhanced markedly when the TNP-nucleotides are located within a more hydrophobic environment, such as when bound to an enzyme active site (*46*−*48*). This effect has enabled use of TNP-ATP as a spectroscopic probe in investigations of binding interactions of ATP with several protein kinases (*49*, *50*), as well as with ATPases (*47*, *51*, *52*), myosin (*48*), and numerous other enzymes and nucleotide binding proteins (*44*, *53*). We used fluorescence spectroscopy to monitor the interaction of TNP-ATP and TNP-ADP with the chemotaxis protein kinase CheA. The fluorescence emission spectrum of TNP-ATP in the presence of CheA (Figure 2A) indicated a severalfold enhancement of the emission intensity and a slight blue-shift of the wavelength of maximal emission. Similar results were obtained with TNP-ADP (Figure 2B).

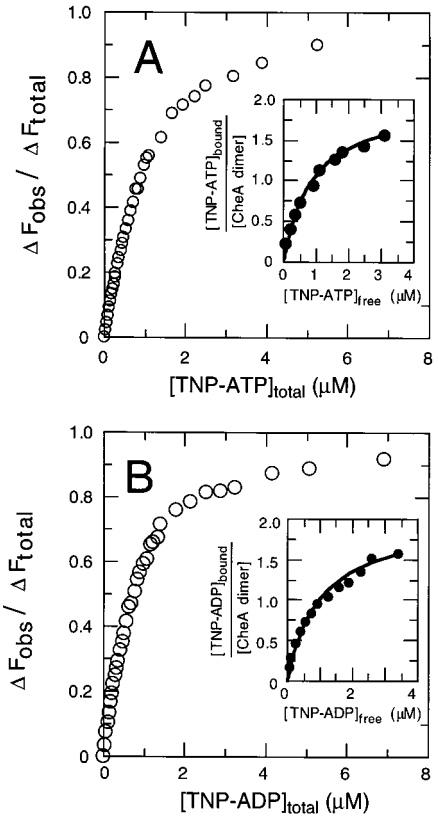

FIGURE 3: Fluorescence-monitored titration of CheA with TNP-ATP and TNP-ADP. (A) successive aliquots of TNP-ATP stock solutions were added to a 3.0 mL sample of CheA (1.0 μM), and the fluorescence intensity (excitation 410 nm, emission 541 nm) was recorded after each addition. Each plotted value represents the difference in fluorescence intensity between the CheA titration and the blank titration and was corrected as described under Experimental Procedures. The data in the main panel were analyzed to generate the binding isotherm shown in the inset. The solid line in this *inset* represents the best fit to the data generated using eq 2 and applying the constraint that $K_{d2} = 4K_{d1}$, as required for two identical, independent sites; this fit indicated a K_{d1} value of 0.44 μM and a K_{d2} value of 1.76 μM (determined by nonlinear least-squares fitting). (B) Titration of CheA with TNP-ADP following the procedures described in (A). The titration curve was analyzed to generate the binding isotherm shown in the inset. In this instance, the best fit was obtained with $K_{d1} = 0.5$ μM and $K_{d2} = 2.0$ μM (identical, independent sites constraint applied).

In the experiments described above, and in the following sections, we used a mutant version of CheA lacking the phosphorylation site (CheA-H48Q) to avoid possible complications that might arise from phosphorylation of the CheA. Previous work has demonstrated that this mutation completely eliminates CheA autophosphorylation (*54*) but does not adversely affect the ability of the kinase active site to bind ATP (*31*) or to trans-phosphorylate the P1 module of a separate CheA subunit (*33*, *55*). In each of the fluorescence experiments described below, we obtained identical results with wild-type CheA and CheA-H48Q. The results for the CheA-H48Q are reported here to eliminate the need to consider any effects of CheA phosphorylation on nucleotide binding.

We monitored the fluorescence intensity of the TNP-nucleotide as we titrated a fixed amount of CheA-H48Q with increasing concentrations of TNP-ATP and TNP-ADP (Figure 3A,B). These data indicated saturable binding. Quantitative analysis of titration data required that we

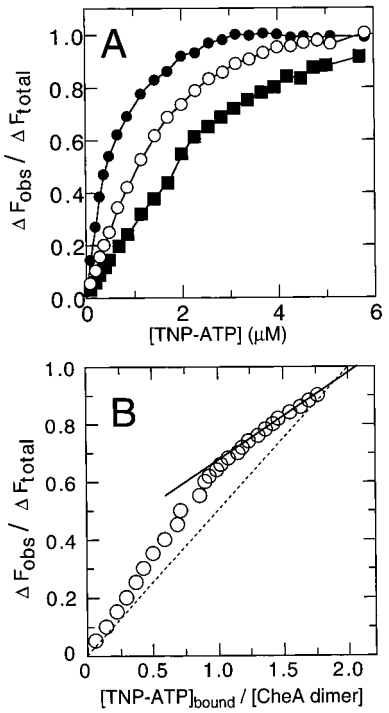

FIGURE 4: Fluorescence-monitored TNP-ATP titrations at three different CheA concentrations. (A) Results of titrations carried out as in Figure 3 but at three different concentrations of CheA-H48Q: (●) 0.76 μM; (○) 2.5 μM; (■) 3.9 μM. The solid lines connecting the data points were added to help the reader to distinguish among the data sets and have no theoretical significance. (B) Relating titration profiles to the average number of TNP-ATP molecules bound per CheA dimer. The data in panel A were analyzed using the approach of Bujalowski et al. (*44*, *45*) to calculate the average concentration of nucleotide bound per CheA dimer at a series of selected values of $\Delta F_{observed}/\Delta F_{total}$. The solid line represents an extrapolation of the linear region observed at the high end of the curve and indicates a binding stoichiometry of 2.1. Three replicates of this same experiment indicated an average stoichiometry of 2.1 $\pm$ 0.2. The dashed line indicates the theoretical situation in which binding of the two molecules of TNP-ATP to the CheA dimer contribute equally to the observed fluorescence change.

determine the stoichiometry of binding and define the relationship between the observed spectral change and nucleotide binding. To define this relationship, we followed the approach of Bujalowski et al. (*44*, *45*) as described under Experimental Procedures. This involved performing fluorescence titrations of CheA with TNP-ATP at three different protein concentrations (Figure 4A). Using the results of these titrations, we defined the relationship between the fractional fluorescence change ($\Delta F_{obs}/\Delta F_{total}$) and the number of TNP-ATP molecules bound per CheA dimer, as shown in Figure 4B. For values of [nucleotide]$_{bound}$/[CheA dimer] above ~1.2, this plot was linear. Extrapolation of this linear region indicated a binding stoichiometry of 2.1 $\pm$ 0.2.

In addition, the curve observed in Figure 4B indicated that the two TNP-ATP molecules bound to the CheA dimer do not contribute equally to the observed spectral change. To further illustrate this point, we included in Figure 4B a dashed line indicating the relationship that would be observed if binding of the first and second nucleotides to the CheA dimer generated equal spectral changes. The data clearly deviate from this dashed line and indicate that binding of the first TNP-ATP generates a greater spectral change than does binding of the second. Similar experiments and analysis

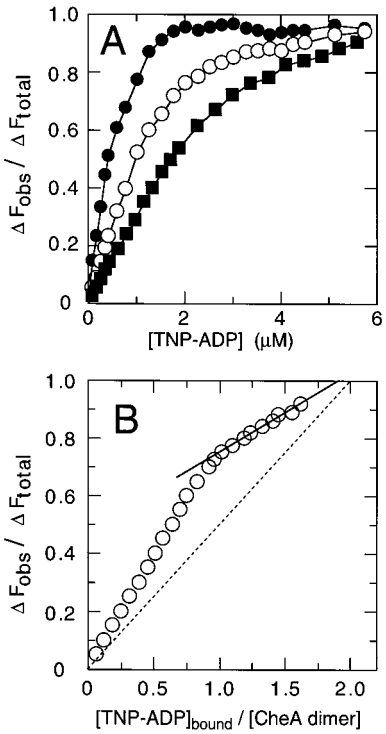

FIGURE 5: Fluorescence-monitored TNP-ADP titrations at three different CheA concentrations. (A) Results of titrations carried out as in Figure 3 but at three different concentrations of CheA-H48Q: (●) 0.76 μM; (○) 2.5 μM; (■) 3.9 μM.. The solid lines connecting the data points were added to help the reader to distinguish among the data sets and have no theoretical significance. (B) Relating titration profiles to the average number of TNP-ADP molecules bound per CheA dimer. The data in panel A were analyzed as in Figure 4. The solid line represents an extrapolation of the linear region observed at the high end of the curve and indicates a binding stoichiometry of 1.9. Three replicates of this same experiment indicated an average stoichiometry of 1.9 ± 0.2. The dashed line indicates the theoretical situation in which binding of the two molecules of TNP-ATP to the CheA dimer contribute equally to the observed fluorescence change.

were performed for titrations of CheA with TNP-ADP (Figure 5A,B), indicating saturation of the CheA binding sites at 1.9 ± 0.2 molecules of TNP-ADP per CheA dimer. These data also indicated a greater fluorescence change for binding of the first of the two molecules of TNP-ADP to the CheA dimer.

The information generated in Figure 4B and Figure 5B enabled us to use titration data (such as in Figure 3) to generate binding isotherms (plots of [nucleotide]$_{bound}$/[CheA dimer] versus [nucleotide]$_{free}$) (*44*). These binding isotherms were then used to estimate the affinity of CheA-H48Q for TNP-ATP and TNP-ADP (e.g., see insets of Figure 3A,B). This involved fitting the binding isotherms using eq 2: binding of the first nucleotide molecule is reflected by the value of dissociation constant K_{d1}, binding of the second nucleotide molecule by K_{d2}. Repeating this analysis for three independent titrations indicated macroscopic dissociation constants $K_{d1} = 0.4 \pm 0.1$ μM and $K_{d2} = 1.8 \pm 0.6$ μM for the binding of TNP-ATP to CheA-H48Q and values of $K_{d1} = 0.4 \pm 0.1$ μM and $K_{d2} = 1.9 \pm 0.9$ μM for the binding of TNP-ADP to CheA-H48Q. Results obtained by following the same procedure with wild-type CheA generated essentially the same values for K_{d1} and K_{d2} (see Table 1). Our results indicated K_{d2} values that were reproducibly 3−5-fold higher than the K_{d1} values. This situation is consistent with the CheA dimer having two identical, independent ATP binding sites (a situation that predicts $K_{d2} = 4K_{d1}$). The computer-generated fits (solid lines) in the insets of Figure 3A,B were generated by constraining eq 2 to require $K_{d2} = 4K_{d1}$.

Table 1: Effects of Mutations on the Affinity of CheA for TNP-ATP and TNP-ADP[a]

CheA variant	TNP-ATP		TNP-ADP	
	K_{d1} (μM)	K_{d2} (μM)	K_{d1}(μM)	K_{d2} (μM)
wild type	0.5 ± 0.1	1.7 ± 0.5	0.4 ± 0.1	1.5 ± 0.7
H48Q	0.4 ± 0.1	1.8 ± 0.6	0.4 ± 0.1	1.9 ± 0.9
G1/G2	125 ± 75	ND	100 ± 60	ND
G470K	0.4 ± 0.1	1.5 ± 0.6	0.5 ± 0.2	1.8 ± 0.7

[a] Dissociation constants (K_d) reflecting the affinity of CheA for TNP-ATP and TNP-ADP were determined by fitting titration data as described for Figure 3. Values are given as the mean ± SE for two or three independent titrations. ND, not determined.

Effects of ADP and ATP on TNP-Nucleotide Binding to CheA. High concentrations of ADP and ATP completely reversed the fluorescence signal associated with formation of the complex between CheA and either TNP-ADP or TNP-ATP (Figure 6A,B). The simplest interpretation of these results is that ATP and ADP compete with TNP-ATP and TNP-ADP for the two nucleotide binding sites of the CheA dimer. Addition of 10 mM $MgCl_2$ enhanced the ability of both ATP and ADP to compete with the TNP-nucleotides. This result suggests that Mg^{2+} enhances the affinity of CheA for ATP and ADP. By contrast, Mg^{2+} appears to have little influence on the affinity of CheA for TNP-ATP and TNP-ADP (data not shown). To obtain a better quantitative understanding of the competition between TNP-ATP and ATP, we titrated a fixed amount of CheA-H48Q with TNP-ATP in the presence of ATP concentrations ranging from 0 to 5 mM (10 mM $MgCl_2$ present in all cases) (Figure 7A). As expected for such a competitive situation (see eq 3), analysis of these data (Figure 7B) indicated a linear relationship between the apparent affinity of CheA for TNP-ATP and the concentration of the competing ligand (ATP). This relationship indicated macroscopic dissociation constants of $K_{d1}^{ATP} = 0.26 \pm 0.05$ mM and $K_{d2}^{ATP} = 1.1 \pm 0.4$ mM for the CheA complexes with Mg^{2+}-ATP. These K_d values were calculated from Figure 7B as discussed under Experimental Procedures. With ADP as the competing nucleotide (Figure 8), analysis of TNP-ADP titration experiments indicated a K_{d1}^{ADP} value of 0.09 mM and K_{d2}^{ADP} value of 0.33 mM. The relative values of K_{d1} and a K_{d2} for the complexes of ATP and ADP with CheA are consistent with the CheA dimer having two identical, independent ATP binding sites. The values of K_{d1}^{ATP} and K_{d1}^{ADP} determined here agree with previous estimates (*31*) obtained by Hummel−Dreyer chromatography (*35*) and are quite close to the K_m values defined by previous kinetics experiments (*30*, *31*). It is important to note that our binding experiments were performed using an unphosphorylatable version of CheA (CheA-H48Q), so there was no possibility that results could be influenced by having a mixed population in which some of the CheA was phosphorylated and some unphosphorylated.

Inhibition of CheA Autokinase Activity by TNP-ATP and TNP-ADP. The steady-state autokinase activity of CheA can be monitored conveniently by coupling ATP consumption (ADP production) to NADH oxidation using an assay

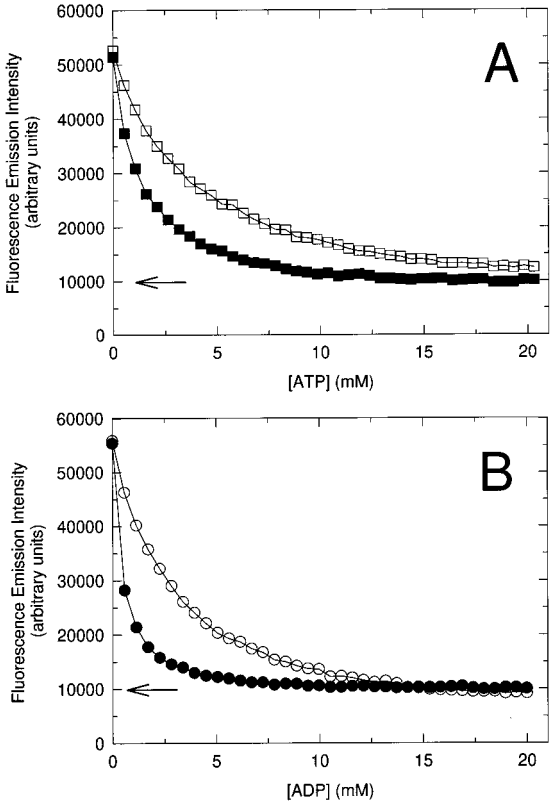

FIGURE 6: Reversal of fluorescence changes at high concentrations of ATP and ADP. (A) Aliquots of ATP were added to a 3.0 mL solution containing 1.0 μM CheA-H48Q and 1.0 μM TNP-ATP in TEDK buffer (□) or TEDKM buffer (■). The arrow indicates the fluorescence emission signal observed for 1.0 μM TNP-ATP in the absence of CheA. (B) Aliquots of ADP were added to a 3.0 mL solution containing 1.0 μM CheA-H48Q and 1.0 μM TNP-ADP in TEDK buffer (○) or TEDKM buffer (●). The arrow indicates the fluorescence emission signal observed for 1.0 μM TNP-ADP in the absence of CheA. Results shown have been corrected for the effects of dilution that resulted from each addition of ATP or ADP. The solid lines connecting the data points in both panels were added to help the reader to distinguish among the data sets and have no theoretical significance.

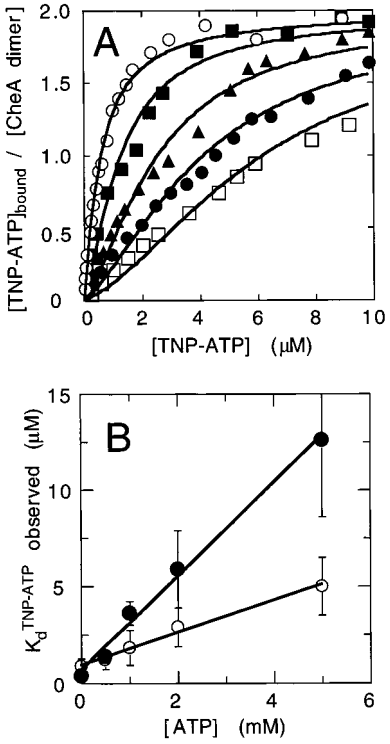

FIGURE 7: Competition between ATP and TNP-ATP for CheA binding sites. (A) TNP-ATP aliquots were added to CheA-H48Q samples (0.75 μM) containing (○) 0 ATP, (■) 0.5 mM ATP, (▲) 1 mM ATP, (●) 2.0 mM ADP, and (□) 5.0 mM ATP. The solid lines are theoretical binding curves calculated for values of K_{d1} and K_{d2} that enabled eq 2 to best fit the data without any further constraints. (B) The apparent dissociation constants [(●) $K_{d1}^{TNP-ATP}$; (○) $K_{d2}^{TNP-ATP}$] for the complexes of CheA with TNP-ATP were plotted as a function of ATP concentration. The *x*-axis intercepts of these plots indicate the values of K_{d1}^{ATP} and K_{d2}^{ATP} (see eq 3). The data plotted in panel B include the $K_d^{TNP-ATP}$ values obtained from analysis of the results in panel A and two replicate experiments.

mixture that includes CheA and CheY as well as L-lactate dehydrogenase, pyruvate kinase, and appropriate substrates (*40*). In the presence of a sufficient level of CheY, CheA autophosphorylation is rate-limiting for ATP turnover (*41*). Using this assay, we monitored the effect of TNP-ATP and TNP-ADP on the steady-state autokinase activity of CheA across a range of ATP concentrations. Both TNP-ATP (Figure 9) and TNP-ADP (Figure 10) served as effective inhibitors of CheA autokinase activity. The results presented in Figure 9A and Figure 10A indicated that TNP-ATP and TNP-ADP served as competitive inhibitors of the interaction of CheA with ATP. Further analysis of the inhibition results indicated a K_i of 0.7 ± 0.2 μM for TNP-ATP (Figure 9B) and a K_i of 0.7 ± 0.2 μM for TNP-ADP (Figure 10B). These K_i values are close to the $K_d^{TNP-ATP}$ and $K_d^{TNP-ADP}$ values obtained by fluorescence titrations (above). At concentrations of TNP-ATP and TNP-ADP higher than 10 μM, the inhibition pattern became more complicated, indicating a mixed inhibition pattern at high concentrations of inhibitor (data not shown). We did not perform an extensive study of inhibition at TNP-nucleotide concentrations above 10 μM, nor did we attempt a detailed analysis of the complex inhibition pattern generated at high inhibitor concentrations.

We used another steady-state assay to assess whether CheA can utilize TNP-ATP as a substrate and become phosphorylated as a result of this interaction. In these assays, we mixed TNP-ATP (20 or 50 μM) with CheA (5 μM), CheY (10 μM), $MgCl_2$ (10 mM), and an enzymatic P_i detection system (*42*). While this system readily detected the P_i generated by turnover of ATP (resulting from the combined action of CheA and CheY), it indicated no detectable turnover of TNP-ATP, even over prolonged time intervals (data not shown). We conclude that TNP-ATP does not appear to serve as a substrate for CheA. Control experiments (data not shown) indicated that TNP-ATP did not inhibit the P_i detection system at these concentrations.

Effects of Mutations in the CheA Transmitter Module. Several catalytically inactive versions of CheA have been generated by mutagenesis and described in previous work (*20*, *26*, *33*, *54*, *56*). We purified two such inactive mutant proteins, confirmed that they lacked autokinase activity (data not shown), and investigated their abilities to bind ADP and ATP using the chromatography method of Hummel and Dreyer (*31*) (Figure 11). One of these mutant proteins (CheA-G1/G2) contained four, site-directed Gly→Ala substitutions affecting both G1 and G2 (*29*); the other mutant protein (CheA-G470K) contained a single Gly→Lys substitution in G2. CheA-G470K was generated by random mutagenesis (*11*) and has been used in previous work for a

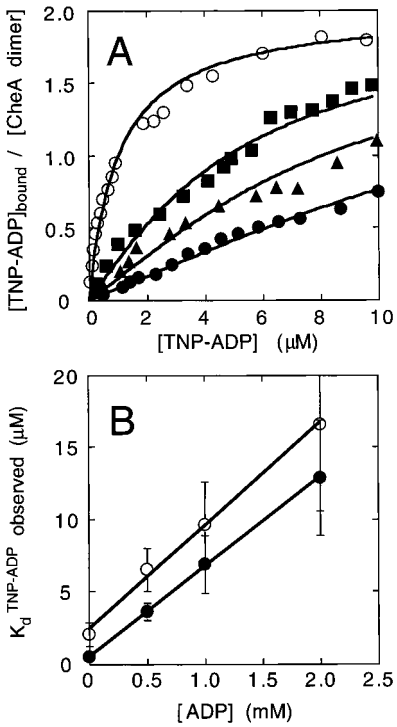

FIGURE 8: Competition between ADP and TNP-ADP for CheA binding sites. (A) TNP-ADP aliquots were added to CheA samples (0.75 μM) containing (○) 0 ATP, (■) 0.5 mM ATP, (▲) 1 mM ATP, and (●) 2.0 mM ADP. The solid lines are theoretical binding curves calculated as described in Figure 7. (B) The effect of ADP concentration on the apparent dissociation constants [(●) $K_{d1}^{TNP-ADP}$; (○) $K_{d2}^{TNP-ADP}$] for the complexes of CheA with TNP-ADP. The *x*-axis intercepts of these plots indicate the values of K_{d1}^{ADP} and K_{d2}^{ADP}. The data plotted in panel B include the $K_d^{TNP-ADP}$ values obtained from analysis of the results in panel A and two replicate experiments.

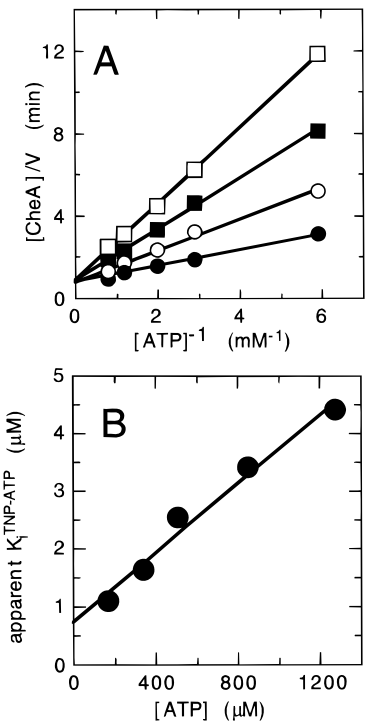

FIGURE 9: TNP-ATP as an inhibitor of CheA autokinase activity. (A) CheA autokinase activity was assayed as described under Experimental Procedures at a series of ATP concentrations (0.17−1.3 mM) and at a series of concentrations of the inhibitor TNP-ATP: (●) 0; (○) 3.3 μM; (■) 6.7 μM; and (□) 9.9 μM. Results were also collected at 0.66, 1.33, 2.0, and 5.0 μM TNP-ATP, but these were not included in panel A to simplify the figure. Solid lines represent best linear fits of these double-reciprocal plots. (B) Dixon plot to analyze the competition between ATP and TNP-ATP. The data from panel A were analyzed to determine the apparent value of $K_i^{TNP-ATP}$ at each concentration of ATP. This was accomplished by fitting a simple hyperbolic binding curve to a plot of percent inhibition versus the concentration of free TNP-ATP (calculated assuming a binding stoichiometry of 2 per CheA dimer). According to eq 3, this plot is expected to have a slope equal to $K_i^{TNP-ATP}/K_m^{ATP}$ and a *y*-axis intercept equal to the true $K_i^{TNP-ATP}$ (i.e., the value in the absence of any competitor ATP).

variety of purposes (*32*, *33*, *55*). Our chromatographic assays indicated that CheA-G1/G2 had a dramatically diminished affinity for ADP (Figure 11) and ATP (data not shown). By contrast, CheA-G470K exhibited affinities for ADP (Figure 11) and ATP (data not shown) that were approximately the same as those exhibited by wild-type CheA and CheA-H48Q.

We used these two mutant proteins as simple test cases to address two fundamental questions that have important implications for assessing whether TNP-ATP is a useful tool to investigate the effects of mutations on CheA's ability to bind unmodified ATP: (1) Does a mutation that disrupts the ability of CheA to bind unmodified ATP also disrupt TNP-ATP binding? (2) Does a mutation that alters the active site of CheA, without disrupting ATP binding, have a similar lack of effect on TNP-ATP binding? Our results (Table 1) indicated that CheA-G470K bound TNP-ATP and TNP-ADP with approximately the same affinity and stoichiometry exhibited by wild-type CheA and CheA-H48Q. By contrast, CheA-G1/G2 had dramatically diminished affinities for TNP-ATP and TNP-ADP. For example, K_{d1} for the complex between TNP-ATP and CheA-G1/G2 was 125 ± 75 μM, a value considerably higher than that observed for the interaction of TNP-ATP with wild-type CheA ($K_{d1} \sim 0.4$ μM). Competition experiments indicated that ATP and ADP competed with the TNP-nucleotides for the ATP binding site of CheA-G1/G2, but the affinity of this mutant protein for ATP and ADP was diminished considerably in much the same way as was observed with the TNP-nucleotides (data not shown). The relatively weak binding of TNP-ATP to CheA-G1/G2 made it difficult to accurately monitor fluorescence changes at ligand concentrations approaching saturating levels because the fluorescence signal due to binding was superimposed on a large background signal (due to unbound TNP-nucleotide) and because the high TNP levels required correspondingly large inner-filter corrections. Because of this situation, we were not able to determine the stoichiometry of nucleotide binding for CheA-G1/G2, and our $K_d^{TNP-ATP}$ and $K_d^{TNP-ADP}$ values for this mutant have large uncertainties (±60−75 μM). Nonetheless, it was clear that the G1/G2 mutations had a pronounced negative effect on the ability of CheA to bind both the unmodified and TNP-modified nucleotides.

For this limited set of mutants, the combined results from the Hummel−Dreyer binding assays and the fluorescence binding assays support the idea that TNP-ATP and TNP-ADP can be used as accurate reporters of the qualitative effects of active site mutations on the ability of CheA to bind unmodified ATP and ADP.

DISCUSSION

Trinitrophenyl derivatives of nucleotides have served as useful tools for characterizing numerous protein kinases and

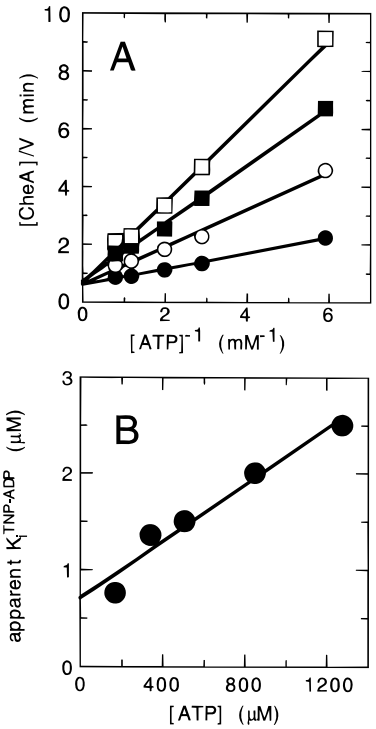

FIGURE 10: TNP-ADP as an inhibitor of CheA autokinase activity. (A) CheA autokinase activity was assayed as described in the legend to Figure 9. Assays contained a range of ATP concentrations (0.17−1.3 mM) and a range of inhibitor (TNP-ADP) concentrations: (●) 0; (○) 1.7 μM; (■) 3.4 μM; (□) 5.1 μM. Results were also collected at 0.85, 2.55, and 4.25 μM TNP-ADP, but these were not included to simplify the figure. Solid lines represent the best linear fits of these double-reciprocal plots. (B) Dixon plot to analyze the competition between ATP and TNP-ADP. The data were analyzed as described for Figure 9.

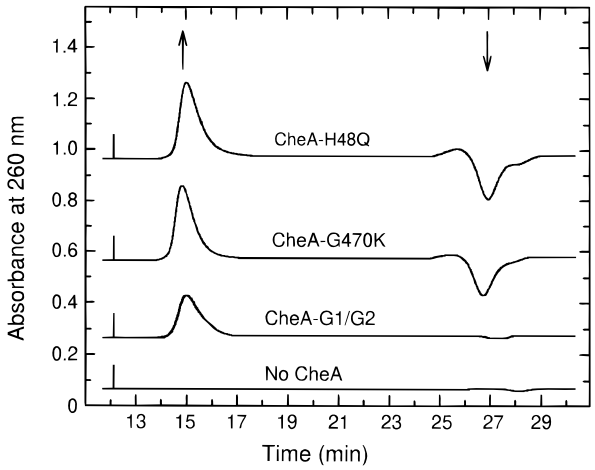

FIGURE 11: Gel filtration chromatography assay of ATP binding by CheA-H48Q, CheA-G470K, and CheA-G1/G2. The procedure described in previous work (*31*) was followed except that a Waters Protein Pak 60 column was used. The column was equilibrated with TEDKM buffer containing 100 μM ADP, and then a 20 μL sample containing 50 μM CheA and 100 μM ADP in TEDKM buffer was injected onto this column. The A_{260} of the eluant was monitored as TEDKM containing 100 μM ADP was pumped through the column following the injection. For CheA samples that bound ADP, a trough was observed in the elution profile at the point where ADP was expected to elute. The area of this trough is an indication of the amount of ADP bound by the CheA, and the similarity of the troughs observed with CheA-G470K and CheA-H48Q indicates that they bind ADP with similar affinities, while the lack of a trough with the CheA-G1/G2 sample indicates a lack of binding. As a control, a 20 μL sample of 100 μM ADP in TEDKM buffer was injected, and the resulting elution profile is labeled as the 'No CheA' sample. The elution profiles were shifted relative to one another along the *y*-axis for the sake of clarity in the figure. When injected separately, CheA eluted at ~15 min postinjection (↑), and ATP eluted at ~27 min postinjection (↓).

nucleotide binding proteins. In particular, use of TNP-ATP as a spectroscopic probe has provided insight into the catalytic mechanisms of ATPases (*47*, *52*, *57*) and, more recently, a tyrosine protein kinase (*49*). In the present work, we examined the interaction of CheA with TNP-ATP and TNP-ADP. To our knowledge, this is the first reported use of these modified nucleotides to characterize a histidine protein kinase. We used fluorescence spectroscopy to monitor this interaction, taking advantage of the enhanced fluorescence properties of the TNP-nucleotides when bound to CheA. Both TNP-ATP and TNP-ADP bound to CheA with high affinity.

Despite the high affinity of TNP-ATP for CheA, this nucleotide analogue does not appear to serve as a substrate for CheA, at least not in a manner that is detectable in steady-state assays requiring multiple turnovers. This observation raises the following question: Is TNP-ATP a valid and useful tool for investigating the binding interactions of CheA with ATP (which does serve as a substrate)? Several other results also suggest that CheA interacts with TNP-ATP somewhat differently than it does with unmodified ATP. Most notably, the affinity of CheA for the TNP-modified nucleotides is several hundred times tighter than for unmodified ATP/ADP. Enhanced affinity for TNP-ATP (relative to unmodified ATP) has been observed with numerous other enzymes, for example, epidermal growth factor receptor (*49*) and sarcoplasmic reticulum Ca^{2+}-ATPase (*57*). Another difference is that Mg^{2+} did not influence the affinity of CheA interactions with TNP-ATP and TNP-ADP. By contrast, Mg^{2+} did influence the affinity of CheA for unmodified ATP and ADP, although Mg^{2+} was not required for this binding. Despite these differences between CheA↔TNP-ATP and CheA↔ATP interactions, there are several important similarities indicating that, in many respects, CheA interactions with TNP-ATP and TNP-ADP are valid indicators of key features of CheA interactions with ATP and ADP. First, the TNP-nucleotides compete with ATP/ADP, presumably because they utilize the same binding sites on the protein. Second, the stoichiometry of binding is the same for TNP-nucleotides and unmodified ATP/ADP; the two binding sites indicated per CheA dimer appear to be identical and noninteracting for both the TNP-modified and the unmodified forms of ATP. And finally, mutations in the presumed ATP binding region of the protein affect binding of TNP-ATP and unmodified ATP in a similar manner. In particular, we demonstrated that altering G1 and G2 disrupted binding of CheA to both TNP-ATP (Table 1) and ATP (Figure 11). Moreover, we demonstrated that TNP-nucleotide titrations accurately reflected the surprising result that the mutant protein CheA-G470K bound ATP with normal affinity (Table 1 and Figure 11). These results indicate that, despite the differences noted above, TNP nucleotides provide an extremely useful spectroscopic probe for further defining the nature of the CheA active site and for exploring the qualitative effects of CheA mutations on ATP binding. It appears likely that binding of TNP-ATP to CheA involves at least some of the same

functional groups as are utilized for binding unmodified ATP to CheA.

The sensitivity of TNP-ATP as a spectral probe of binding events afforded an opportunity to explore the stoichiometry of CheA↔ATP interactions. This binding stoichiometry has considerable significance when considering how CheA operates as an autokinase and how this activity might be regulated by the chemotaxis receptor proteins (*13*, *14*, *58*). However, previous efforts to establish the number of ATP binding sites per CheA dimer were not conclusive, but rather were consistent with either one or two sites per CheA dimer (*31*). As an apparently symmetric dimer, CheA might be expected to have two active sites. The results presented here support this idea. Specifically, we observed a binding stoichiometry of 2 ATP molecules per CheA dimer. Moreover, our results are consistent with the proposal that the CheA dimer has two identical, noninteracting ATP binding sites. It should be noted, however, that for situations where K_{d1} and K_{d2} are less than 10-fold different, it is inherently difficult to accurately assess their individual values (*59*). The resulting uncertainty in our estimates of K_{d1} and K_{d2} means that we cannot rule out the possibility that ATP binding sites 1 and 2 interact weakly.

The stoichiometry of ATP binding to CheA and the approximate affinity of the two binding sites for ATP are useful pieces of information for formulating ideas about how the CheA dimer operates to accomplish autophosphorylation. Both subunits of the dimer become phosphorylated (*31*, *60*), but it is not clear whether this represents one active site phosphorylating two P1 modules in succession or two active sites acting independently, each phosphorylating one of the two P1 modules. The following question remains: Does the CheA dimer have one or two functional active sites? Our results indicate that there are two ATP binding sites, and the simplest extension of this observation would be to propose that there are two distinct kinase active sites per CheA dimer. As discussed above, statistical considerations dictate that two such sites will appear to have different affinities for ATP ($K_{d2} = 4K_{d1}$). In considering the possibility that both ATP binding sites contribute to CheA autophosphorylation, it is useful to compare our values of K_{d1}^{ATP} and K_{d2}^{ATP} to the value of K_m^{ATP} measured previously for the CheA autophosphorylation reaction (*30*, *31*). If both binding sites contribute to autophosphorylation, then K_m^{ATP} should reflect an affinity intermediate between K_{d1}^{ATP} and K_{d2}^{ATP}. However, we find that K_m^{ATP} (0.29 ± 0.04 mM) matches very well with K_{d1}^{ATP} (0.26 ± 0.05 mM) and does not fall within a range intermediate between K_{d1}^{ATP} and K_{d2}^{ATP}. This agreement suggests that the CheA dimer might utilize only one of its two hypothetical active sites or that it might utilize only one active site at a time. In such a 'half-of-sites' situation, the dependence of the kinase activity on the ATP concentration would reflect K_{d1}. Such a situation could arise if interaction of one P1 module with active site 1 prevents interaction of the second P1 module with active site 2: only when the first P1 module has been phosphorylated and cleared out of the active site region can the second P1 module interact with the second active site. Levit et al. (*21*) have previously discussed this possibility and presented supporting kinetic evidence indicating that the two P1 modules in a CheA dimer compete for access to the CheA active site(s).

Another related scenario that would result in apparent 'half-of-sites activity' would be for CheA to have only one kinase active site but two ATP binding sites. For example, the kinase active site might be considerably more complex than the ATP binding site because it must also include a site to bind/orient P1 as well as groups involved in catalyzing the chemistry of phospho-transfer from ATP to His^{48}. Despite the presence of two ATP binding sites, the other components of the active site might be present in only one copy per CheA dimer if, for example, both subunits of the CheA dimer contributed to these components (*32*).

The kinase active site of CheA is thought to involve several regions that are largely conserved in the histidine protein kinase family (*4*, *17*). Two of these regions (G1 and G2) are glycine-rich segments that may function in a manner similar to the multifunctional glycine clusters in several well-characterized protein kinases and nucleotide binding proteins (*22*−*25*). Previous characterization of the effects of site-directed mutations has indicated that G1 and G2 are required for CheA autokinase activity (*26*). The loss of autokinase activity observed in CheA G1 mutants and G2 mutants could arise from a number of effects, including: (i) an inability of the kinase active site to bind ATP; (ii) an inability of the active site to bind the P1 module containing the His^{48} phosphorylation site; (iii) an inability of the active site to catalyze phosphoryl transfer from bound ATP; and (iv) an inability to form dimers. In the work reported here, we investigated whether simultaneously altering G1 and G2 affected the ability of CheA to bind ATP. We found that a combination of glycine-to-alanine substitutions altering both G1 and G2 dramatically reduced the ability of CheA to bind TNP-ATP, TNP-ADP, ATP, and ADP. Thus, G1 and/or G2 appear to be important for CheA binding interactions with ATP and ADP. However, it is worth emphasizing that the mutations in G1/G2 did not completely eliminate binding of ATP (or TNP-ATP) to CheA. Nonetheless, CheA-G1/G2 was completely inactive in autokinase assays (*26*), and this defect could not be corrected by using high concentrations of ATP (VanBruggen and Stewart, unpublished observations). Therefore, the glycine-rich regions of CheA appear to play an important catalytic role in addition to participating in ATP binding.

We were surprised to find that a mutation in the G2 region of CheA (G470K) exerted no apparent effect on CheA binding interactions with ATP and ADP (Figure 11). This phenotype was faithfully reproduced in the titrations of CheA-G470K with TNP-modified ATP and ADP (Table 1). Previous work demonstrated that the Gly^{470}→Lys mutation completely eliminates CheA autokinase activity but does not disrupt the ability of CheA to form dimers (*33*, *55*). Therefore, it appears that Gly^{470} plays an important role in enabling phosphoryl transfer from ATP to His^{48} or in P1 docking to the CheA kinase active site, but it is not required for ATP binding. This mutant protein has been used extensively as a phospho-acceptor in so-called 'trans-phosphorylation' experiments in which, for example, a heterodimer is generated by pairing a kinase-defective CheA mutant (e.g., CheA-G470K) with a version of CheA that is incapable of accepting a phosphate (e.g., CheA-H48Q) (*32*, *33*, *55*). CheA-G470K becomes phosphorylated under these conditions, and this has been attributed to 'trans-phosphorylation' in which the active site of the CheA-H48Q subunit

of the heterodimer (CheA-H48Q/CheA-G470K) directs phosphorylation of the phospho-accepting histidine side chain of the CheA-G470K subunit. Our current results indicate that CheA-G470K may not be a completely passive player in such situations as it binds ATP with normal affinity and therefore might contribute at least this ability to the 'trans-phosphorylation.'

Clearly, there remains much to be learned about how CheA and other HPKs operate. With the goal of further defining the nucleotide binding site of CheA, we are currently making use of TNP-nucleotides and systematic mutagenesis of the conserved transmitter elements of CheA. TNP-nucleotides may provide a useful tool for exploring other histidine protein kinases as well.

ACKNOWLEDGMENT

We thank Sandy Parkinson for providing *E. coli* strains; Kenji Oosawa and Mel Simon for *cheA-501*; Beth Gantt, Steve Wolniak, and the UMCP Plant Biology Department for instrument access during early stages of this work; and the anonymous reviewers for useful comments and suggestions.

REFERENCES

1. Alex, L. A., and Simon, M. I. (1994) *Trends Genet. 10*, 133−138.
2. Alex, L. A., Borkovich, K. A., and Simon, M. I. (1996) *Proc. Natl. Acad. Sci. U.S.A. 93*, 3416−3421.
3. Maeda, T., Wurgler-Murphy, S., and Saito, H. (1994) *Nature 369*, 242−245.
4. Parkinson, J. S., and Kofoid, E. C. (1992) *Annu. Rev. Genet. 26*, 71−112.
5. Schuster, S. C., Noegel, A. A., Oehme, F., Gerisch, G., and Simon, M. I. (1996) *EMBO J. 15*, 3880−3889.
6. Swanson, R. V., Alex, L. A., and Simon, M. I. (1994) *Trends Biochem. Sci. 19*, 485−490.
7. Wang, N., Shaulsky, G., Escalente, R., and Loomis, W. F. (1996) *EMBO J. 15*, 3890−3898.
8. Sanders, D. A., Gillece-Castro, B. L., Stock, A. M., Burlingame, A. L., and Koshland, D. E., Jr. (1989) *J. Biol. Chem. 264*, 21770−21778.
9. Kofoid, E. C., and Parkinson, J. S. (1988) *Proc. Natl. Acad. Sci. U.S.A. 85*, 4981−4985.
10. Hess, J. F., Oosawa, K., Kaplan, N., and Simon, M. I. (1988) *Cell 53*, 79−87.
11. Oosawa, K., Hess, J. F., and Simon, M. I. (1988) *Cell 53*, 89−96.
12. Welch, M., Oosawa, K., Aizawa, S.-I., and Eisenbach, M. (1993) *Proc. Natl. Acad. Sci. U.S.A. 90*, 8787−8791.
13. Borkovich, K. A., Kaplan, N., Hess, J. F., and Simon, M. I. (1989) *Proc. Natl. Acad. Sci. U.S.A. 86*, 1208−1212.
14. Ninfa, E. G., Stock, A., Mowbray, S., and Stock, J. (1991) *J. Biol. Chem. 266*, 9764−9770.
15. Berg, H. C. (1988) *Cold Spring Harbor Symp. Quant. Biol 53*, 1−9.
16. Macnab, R. M. (1987) in *Escherichia coli and Salmonella typhimurium*: *Cellular and molecular biology* (Neidhardt, F. C., et al., Eds.) Vol. 1, pp 732−759, ASM Press, Washington, DC.
17. Stock, J. B., and Surette, M. G. (1996) in *Escherichia coli and Salmonella typhimurium*: *Cellular and molecular biology* (Neidhardt, F. C., et al., Eds.) 2nd ed., Vol. 1, pp 1103−1129, ASM Press, Washington, DC.
18. McEvoy, M. M., Zhou, H., Roth, A. F., Lowry, D. L., Morrison, T. B., Kay, L. E., and Dahlquist, F. W. (1995) *Biochemistry 34*, 13871−13880.
19. Morrison, T. B., and Parkinson, J. S. (1994) *Proc. Natl. Acad. Sci. U.S.A. 91*, 5485−5489.
20. Swanson, R. V., Schuster, S. C., and Simon, M. I. (1993) *Biochemistry 32*, 7623−7629.
21. Levit, M., Liu, Y., Surette, M., and Stock, J. (1996) *J. Biol. Chem. 271*, 32057−32063.
22. Bossenmeyer, D. (1994) *Trends Biochem. Sci. 19*, 201−205.
23. Saraste, M., Sibbald, P. R., and Wittinghofer, A. (1990) *Trends Biochem. Sci. 15*, 430−434.
24. Schulz, G. E. (1992) *Curr. Opin. Struct. Biol. 2*, 61−67.
25. Taylor, S. S., Knighton, D. R., Zheng, J., Ten Eyck, L. F., and Sowadski, J. M. (1992) *Annu. Rev. Cell Biol. 8*, 429−462.
26. Ellefson, D. D., Weber, U., and Wolfe, A. J. (1997) *J. Bacteriol. 179*, 825−30.
27. Ninfa, E. G., Atkinson, M. R., Kamberov, E. S., and Ninfa, A. J. (1993) *J. Bacteriol. 175*, 7024−7032.
28. Yang, Y., and Inouye, M. (1993) *J. Mol. Biol. 231*, 335−342.
29. Wolfe, A. J., McNamara, B. P., and Stewart, R. C. (1994) *J. Bacteriol. 176*, 4483−4491.
30. Surette, M. G., Levit, M., Liu, Y., Lukat, G., Ninfa, E. G., Ninfa, A., and Stock, J. B. (1996) *J. Biol. Chem. 271*, 939−945.
31. Tawa, P., and Stewart, R. C. (1994a) *Biochemistry 33*, 7917−7924.
32. Tawa, P., and Stewart, R. C. (1994b) *J. Bacteriol. 176*, 4210−4218.
33. Wolfe, A. J., and Stewart, R. C. (1993) *Proc. Natl. Acad. Sci. U.S.A. 90*, 1518−1522.
34. Gegner, J. A., and Dahlquist, F. W. (1991) *Proc. Natl. Acad. Sci. U.S.A. 88*, 750−754.
35. Hummel, J. P., and Dreyer, W. J. (1962) *Biochim. Biophys. Acta 63*, 530−532.
36. Hiratsuka, T., and Uchida, K. (1973) *Biochim. Biophys. Acta 320*, 635−647.
37. Studier, F. W., Rosenberg, A. H., Dunn, J. J., and Dubendorff, J. W. (1990) *Methods Enzymol. 185*, 60−89.
38. Stewart, R. C. (1997) *Biochemistry 36*, 2030−2040.
39. Gill, S. C., and von Hippel, P. H. (1989) *Anal. Biochem. 182*, 319−326.
40. Norby, J. G. (1988) *Methods Enzymol. 156*, 116−119.
41. Lukat, G. S., Lee, B. H., Mottonen, J. M., Stock, A. M., and Stock, J. B. (1991) *J. Biol. Chem. 266*, 8348−8354.
42. Webb, M. R. (1992) *Proc. Natl. Acad. Sci. U.S.A. 89*, 4884−4887.
43. Ward, L. D. (1985) *Methods Enzymol. 117*, 400−414.
44. Bujalowski, W., and Klonowska, M. M. (1993) *Biochemistry 32*, 5888−5900.
45. Bujalowski, W., and Lohman, T. M. (1987) *Biochemistry 26*, 3099−3106.
46. Broglie, K. E., and Takahashi, M. (1983) *J. Biol. Chem. 258*, 12940−12946.
47. Grubmeyer, C., and Penefsky, H. S. (1981) *J. Biol. Chem. 256*, 3718−3727.
48. Hiratsuka, T. (1982) *Biochim. Biophys. Acta 719*, 509−517.
49. Cheng, K., and Koland, J. G. (1996) *J. Biol. Chem. 271*, 311−318.
50. Thomas, P. J., Shenbagamurthi, P., Ysern, X., and Perderson, P. L. (1991) *Science 251*, 555−557.
51. Weber, J., and Senior, A. E. (1996) *J. Biol. Chem. 271*, 3474−3477.
52. Faller, L. D. (1990) *Biochemistry 29*, 3179−3186.
53. Van der Wolk, J. P. W., Klose, M., de Wit, J. G., den Blaauwen, T., Freudl, R., and Driessen, A. J. M. (1995) *J. Biol. Chem. 270*, 18975−18982.
54. Hess, J. F., Bourret, R. B., and Simon, M. I. (1988) *Nature (London) 336*, 138−143.
55. Swanson, R. V., Bourret, R. B., and Simon, M. I. (1993) *Mol. Micriobiol. 8*, 435−441.
56. Oosawa, K., Hess, J. F., and Simon, M. I. (1988) *Cell 53*, 89−96.
57. Moutin, M.-J., Cuillel, M., Rapin, C., Miras, R., Anger, M., Lompré, A.-M., and Dupont, Y. (1994) *J. Biol. Chem. 269*, 11147−11154.
58. Borkovich, K. A., and Simon, M. I. (1992) *Cell 63*, 1339−1348.
59. Dahlquist, F. W. (1978) *Methods Enzymol. 48*, 270−299.
60. Hess, J. F., Oosawa, K., Matsumura, P., and Simon, M. I. (1987) *Proc. Natl. Acad. Sci. U.S.A. 84*, 7609−7613.

BI980970N